Turkish Journal of Engineering
https://dergipark.org.tr/en/pub/tuje
e-ISSN 2587-1366

Design and walking analysis of proposed four-legged glass cleaning robot

Nihat Çabuk *[1]

[1]*Aksaray University, Vocational School of Technical Sciences, Türkiye*

Keywords
Serial manipulator
Legged-robot
Glass cleaning
Design
Kinematic analysis

Research Article
DOI: 10.31127/tuje.1011320

Received: 18.10.2021
Accepted: 29.03.2022
Published: 26.04.2022

Abstract

In this study, a legged and wheeled robot model was proposed for cleaning the glass of greenhouses. The robot has four wheels and four legs, each with three degrees of freedom (DOF). The design, kinematic analysis and simulation of the robot was carried out. Glass greenhouses are created by placing glass sheets on T-shaped iron bars arranged in parallel at certain intervals. The robot performs the glass cleaning task by performing two different movements on greenhouse roof. As a first movement, the robot moves like a train moving on the rail on iron bars with wheels, cleaning the glass as it travels. After cleaning the glasses placed between two iron bars along a column, as second movement, the robot passes the next column using legs. These two movements continue until the entire roof of the greenhouse is cleaned. Kinematic analysis of this robot, which is designed with mechanical properties that can make these movements, has been made. Walking simulation of the robot was carried out according to the kinematic analysis. The simulation results showed that this proposed robot can be used to clean glass on the greenhouse roof.

1. Introduction

The use of robots is increasing day by day in parallel with the technological developments in robot components such as sensors, electric motors and controllers. This increase has led to the need for robots to be categorized into some of their features. The classification of robots can made according to many criteria such as whether they move or not, where they are used, drive systems and the structures of their arms or legs. [1-7]. These classifications can be further reproduced according to different characteristics. Studies on all these classifications can be found in the literature [8-9]. These studies can be on both design and control according to the usage areas of the robots [10]. Deng et al. [11] have proposed several methods for hexapod robots to overcome object handling problems by using one or both legs as an arm when walking on other legs. Robots are also an important part of agricultural activities such as fertilizing and spraying as well as planting and harvesting [12-14]. Ling et al. [15] developed a mobile robot to tomato harvesting. This robot, which has two arms, each with two degrees of freedom (DOF), also has a sensor that detects tomatoes.

It is also possible to find studies for general cleaning [16] and cleaning glass in buildings [17]. Sun et al. [18] designed a climbing robot to clean glasses for high rise buildings. Their robot has suction cups to stick on the glass and it moves with a translation mechanism. Antonelli et al. [19] carryout an experimental study on cleaning robot to clean dust on solar photovoltaic panels in solar plants. Li et al. [20] explored different greenhouse cleaning machines. Also, they analyzed the current state of development and prospects of greenhouse cleaning equipment and made some suggestions. Seemuang [21] study on cleaning mechanism to clean roof of plastic sheeting greenhouse.

According to the literature searches, no study has been found on a robot that performs the task of cleaning the glass of greenhouses. Therefore, in this study, a four-legged and four-wheeled mobile robot that cleans the glass of greenhouse roofs was designed, kinematic analysis was performed and simulation was carried out.

* **Corresponding Author**
*(nihatcabuk@aksaray.edu.tr) ORCID ID 0000-0002-3668-7591

Cite this article
Çabuk, N. (2023). Design and walking analysis of proposed four-legged glass cleaning robot. Turkish Journal of Engineering, 7(2), 82-91

This study consists of the following sections. In the following section, the structural features of the greenhouses were examined and the reason for this study was explained. Next, a solid model of a greenhouse was created and associated with the designed robot and the physical properties of the robot were determined in accordance with the field of use and purpose and a solid model was created. Besides, mathematical equations were obtained by performing kinematic analysis according to this model. In the third section, the robot's walking simulation was performed and its applicability in a real environment was evaluated. In the fourth section, the study was concluded.

2. Method

2.1. Problem overview

Glass greenhouses are structures that can take sunlight well, where air conditioning can be done very well. Although these greenhouses differ according to the region, they are closed areas where fruits and mostly vegetables are grown in cold weather conditions. As it is known, it is an important issue that the glass of these greenhouses, which has a structure that permits sunlight, which is one of the most basic needs of plants although some plants may decrease their yields if exposed to intense sunlight to be transparent in order to pass this light sufficiently, especially in winter. Although it is partially cleaned due to the rain during the year, the cleaning of these glasses, whose transparency decreases over time due to various reasons, is also important due to the reasons mentioned above.

Glass greenhouses are formed by placing certain sizes of glass layers on grids of iron bars (T shape). These glass sheets are generally 550x600 and 500x550 mm in size. Fig. 1 shows a general glass greenhouse subject to this study.

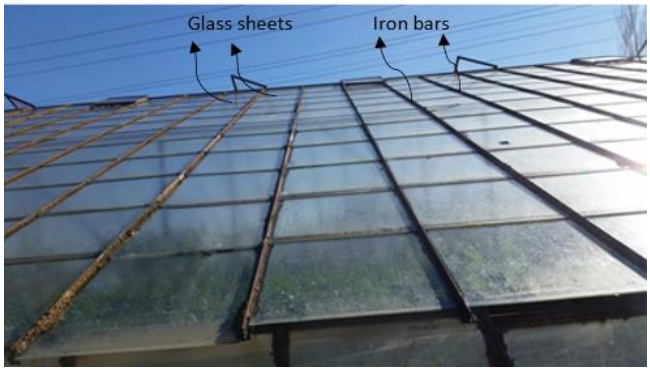

Figure 1. Glass greenhouse structure

2.2. Cleaning strategy

The designed robot has four legs and four wheels. While the wheels enable the robot to move on two fixed iron bars, similar to the movement of the train on the rails, the four legs enable the robot to pass on the other two iron bars. The direction of movement of the robot with wheels and the direction of movement with legs can be seen in Fig. 2.

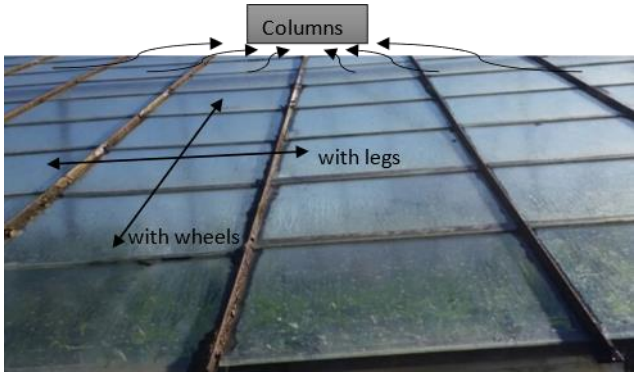

Figure 2. Motion directions of the robot on greenhouse roof

The glass is cleaned with the rotating brush on the robot body and the water coming from the water hose connected externally to the robot. After one column is completely cleaned by the movement of the wheels, the robot moves to the other column by its legs. Both legs and wheels are driven by electric motors. In addition to these, since the brushing system is operated by an electric motor, the electrical energy needed by the robot will be quite high. Thus, this energy is not provided by a battery, but by a cable connected to the electricity grid.

The angle of inclination of the iron bars forming the roof of greenhouses is usually between 20 and 30 degrees in practice. The section view of the greenhouse solid model created by selecting this angle as approximately 30 degrees is given in Fig. 3. Although this angle is a variable that affects the motion of the robot, this study does not include dynamic analysis involving the motion of the robot.

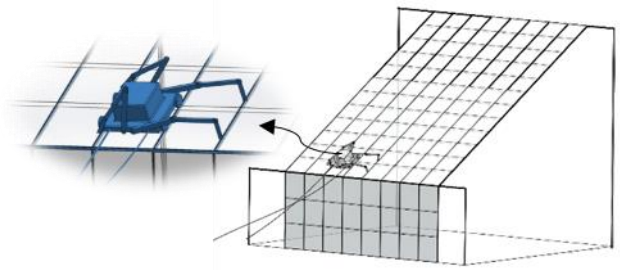

Figure 3. Solid model the greenhouse section and the robot on roof

The serial manipulators that make up the structure of the robot designed within the scope of this study are the mechanisms used in both any legged robot and industrial robot arms. The fields of use can be diversified by adding the required equipment according to the purpose and place of use [22-26].

Each limb of serial manipulators is connected one after the other. These connections are made with rotary, spherical or prismatic joints. The robot designed in this study has serial manipulators and rotational joints are used in these manipulators. The most common example of the use of serial manipulators is industrial robot arms. In these robot arms, the limbs connected to each other by joints, the limb in the base frame and the limb farthest from the base frame and the end actuator is always the same task. Thus, the kinematic chain of the manipulator is formed from the base frame to the end effector fame.

In robots where serial manipulators are used, kinematic analysis of the manipulator should be performed in order to define the robot's motion mathematically. The complexity of this kinematic equation increases as the degree of freedom of the manipulator increases and the rotation axes of the successive joints differ. Kinematic analysis is carried out in two ways: forward kinematics, where the positions of the manipulator's limbs can be determined according to the angle value of the joints and the dimensions of the limbs, and inverse kinematics, where the required joint angles for the desired position and orientation of the limbs are determined. The position relation between the limbs of manipulators that can move in three axes can be established by writing in matrix form using the coordinate axis sets assigned to the joints, while this relationship can be established more simply in planar manipulators moving in two axes. Equation 1 is the forward kinematic equation of a 3-DOF planar manipulator.

$$P_x = l_1\cos(\theta_1) + l_2\cos(\theta_1+\theta_2) + l_3\cos(\theta_1+\theta_2+\theta_3)$$
$$P_y = l_1\sin(\theta_1) + l_2\sin(\theta_1+\theta_2) + l_3\sin(\theta_1+\theta_2+\theta_3) \quad (1)$$

Here, θ_1 is the angle between the reference axis of the first limb of the serial manipulator, θ_2 is the angle between the the second limb and the axis of first limb and θ_3 is the angle between the third limb and the axis of second limb. Similarly, l_1, l_2 and l_3 are the lengths of the first, second and third limb of the manipulator, respectively. Besides, P_x and P_y are the coordinates of the manipulator's endpoint. In the following section, kinematic analysis of a four-legged robot, each consisting of 3-DOF planar manipulators, is performed.

2.3. Mechanical design

This proposed four-legged robot basically consists of four serial manipulators with 3-DOF. These legs serve to carry the robot body to the iron bar on one side. In addition, it has four wheels driven by an electric motor that move the robot body on iron bars as seen in Fig. 2 and Fig. 3. The roller brush placed under the body of the robot cleans the glass while moving in the same column with the robot wheels. The water required in this cleaning process is provided by the water hose connected to the robot body. Similarly, the electrical energy needed by the robot is transmitted to the robot with the power cable. The motor drivers, power supply and control unit required for the electric motors which are in leg joints, drive the wheels and rotating the brush are in the chamber on the robot as seen in Fig. 4.

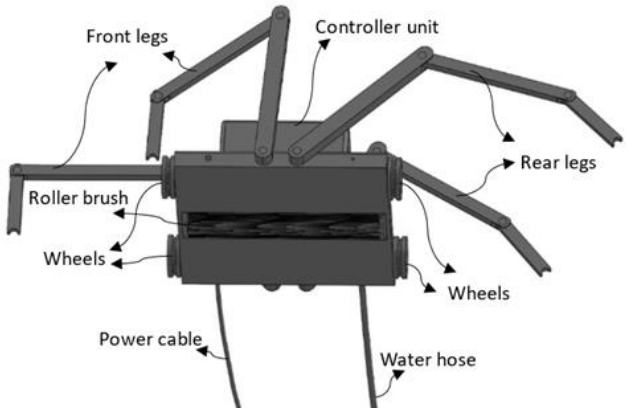

Figure 4. Components of the cleaning robot

In order to obtain the kinematic equations of the robot, the physical description of the robot body is made in Fig. 5. Since the other two legs of the robot are the same as these two legs, it is not shown in this figure.

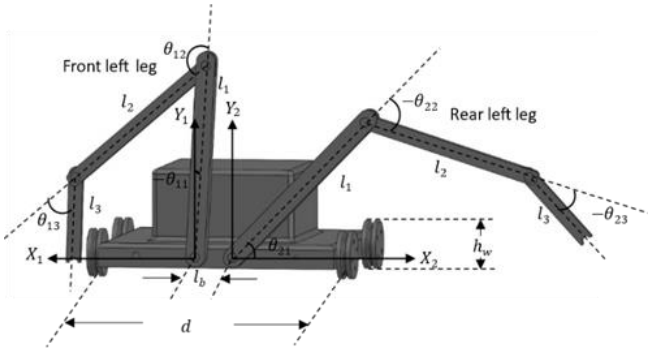

Figure 5. The cleaning robot structure

Here, d is the distance between the two wheels and also represents the distance between the two iron bars. h_w is the diameter of the wheel and l_b is the distance between the axes of rotation of the first joints of the front and rear legs. l_1, l_2 and l_3 are length of leg limbs. θ_{11} is the angle between the reference axis of the first limb of the serial manipulator, θ_{12} is the angle between the the second limb and the axis of first limb and θ_{13} is the angle between the third limb and the axis of second limb for front legs. θ_{21}, θ_{22} and θ_{23} represent the same variables for the rear legs. Although the installation of greenhouses is made to certain standards, the dimensions of the robot body and legs should be adjustable in accordance with the greenhouse structure in general.

2.4. Kinematic analysis

In this study, the base frame and the end effector frame change places at every step of the robot. Thus, two different kinematic chains are used to obtain the kinematic equation of the robot [27]. Fig. 6 shows the robot kinematic configuration and axes defined for kinematic analysis.

Here, $\boldsymbol{G}$-axis set fixed to the body center of gravity can move freely in space with the body. The transformation matrix defining the configuration of the $\boldsymbol{G}$ axis set according to the axis set $\widehat{\boldsymbol{G}}$ which is located at any point in the robot's motion trajectory is given in equations 2-5. Here, T_{trans} is translational vector of these two axis sets. The rotation matrix $R_{r,p,y}$ denotes the orientation of the $\mathbf{G}$ axis set with respect to the axis set $\widehat{\boldsymbol{G}}$. And the

orientation is defined by the roll-pitch-yaw angular representation.

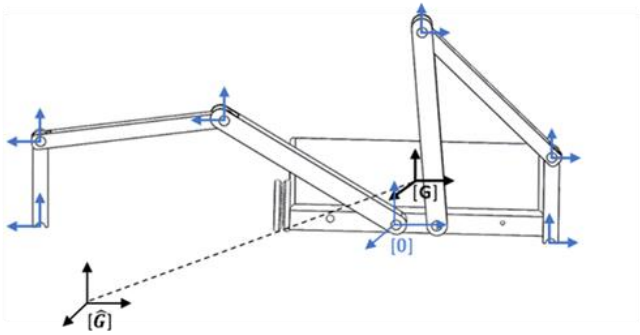

Figure 6. Placement of axis sets on the robot

$$T_{trans} = [x_{\hat{G}}\ y_{\hat{G}}\ z_{\hat{G}}] \tag{2}$$

$$R_p = \begin{bmatrix} \cos(pitch) & -\sin(pitch) & 0 \\ \sin(pitch) & \cos(pitch) & 0 \\ 0 & 0 & 1 \end{bmatrix} \tag{3a}$$

$$R_y = \begin{bmatrix} \cos(yaw) & \sin(yaw) & 0 \\ 0 & 1 & 0 \\ -\sin(yaw) & \cos(yaw) & 0 \end{bmatrix} \tag{3b}$$

$$R_r = \begin{bmatrix} 1 & 0 & 0 \\ 0 & \cos(roll) & -\sin(roll) \\ 0 & \sin(roll) & \cos(roll) \end{bmatrix} \tag{3c}$$

$$R_{r,p,y} = R_p * R_y * R_r \tag{4}$$

$${}^{\hat{G}}T_G = \begin{bmatrix} R_{r,p,y} & T_{trans}^T \\ 0_{[1x3]} & 1 \end{bmatrix} \tag{5}$$

Subsequently, the configurations of the leg fixed axis sets according to the G axis set can be expressed as in equation 6. Here, LF, RF, LR and RR represent the left front, right front, left rear and right rear legs respectively.

$${}^{G}_{0}T^{LF} = \begin{bmatrix} \cos(\frac{\pi}{2}) & 0 & \sin(\frac{\pi}{2}) & -\frac{d}{2} \\ 0 & 1 & 0 & 0 \\ -\sin(\frac{\pi}{2}) & 0 & \cos(\frac{\pi}{2}) & \frac{l_b}{2} \\ 0 & 0 & 0 & 1 \end{bmatrix} \tag{6a}$$

$${}^{G}_{0}T^{RF} = \begin{bmatrix} \cos(\frac{\pi}{2}) & 0 & \sin(\frac{\pi}{2}) & \frac{d}{2} \\ 0 & 1 & 0 & 0 \\ -\sin(\frac{\pi}{2}) & 0 & \cos(\frac{\pi}{2}) & \frac{l_b}{2} \\ 0 & 0 & 0 & 1 \end{bmatrix} \tag{6b}$$

$${}^{G}_{0}T^{LR} = \begin{bmatrix} \cos(-\frac{\pi}{2}) & 0 & \sin(-\frac{\pi}{2}) & \frac{d}{2} \\ 0 & 1 & 0 & 0 \\ -\sin(-\frac{\pi}{2}) & 0 & \cos(-\frac{\pi}{2}) & -\frac{l_b}{2} \\ 0 & 0 & 0 & 1 \end{bmatrix} \tag{6c}$$

$${}^{G}_{0}T^{RR} = \begin{bmatrix} \cos(-\frac{\pi}{2}) & 0 & \sin(-\frac{\pi}{2}) & -\frac{d}{2} \\ 0 & 1 & 0 & 0 \\ -\sin(-\frac{\pi}{2}) & 0 & \cos(-\frac{\pi}{2}) & -\frac{l_b}{2} \\ 0 & 0 & 0 & 1 \end{bmatrix} \tag{6d}$$

With a similar approach, the configurations of the axis set placed at the other joints of the legs can be expressed as in equation 7. Finally, the transformation matrices describing the configuration of the axes placed at the end points of the robot legs with respect to the ***G*** axis set can be found as in equation 8. Subsequently, the transformation matrices describing the configuration of the leg endpoints with respect to the **0** inertial axes set can be found as in equation 9. Thus, forward kinematic equations of the robot were obtained.

$${}^{0}_{1}T = \begin{bmatrix} \cos(\theta_{11}) & -\sin(\theta_{11}) & 0 & l_1\cos(\theta_{11}) \\ \sin(\theta_{11}) & \cos(\theta_{11}) & 0 & l_1\sin(\theta_{11}) \\ 0 & 0 & 1 & 0 \\ 0 & 0 & 0 & 1 \end{bmatrix} \tag{7a}$$

$${}^{1}_{2}T = \begin{bmatrix} \cos(\theta_{12}) & -\sin(\theta_{12}) & 0 & l_2\cos(\theta_{12}) \\ \sin(\theta_{12}) & \cos(\theta_{12}) & 0 & l_2\sin(\theta_{12}) \\ 0 & 0 & 1 & 0 \\ 0 & 0 & 0 & 1 \end{bmatrix} \tag{7b}$$

$${}^{2}_{3}T = \begin{bmatrix} \cos(\theta_{13}) & -\sin(\theta_{13}) & 0 & l_3\cos(\theta_{13}) \\ \sin(\theta_{13}) & \cos(\theta_{13}) & 0 & l_3\sin(\theta_{13}) \\ 0 & 0 & 1 & 0 \\ 0 & 0 & 0 & 1 \end{bmatrix} \tag{7c}$$

$${}^{0}_{3}T = {}^{0}_{1}T\ {}^{1}_{2}T\ {}^{2}_{3}T \tag{8}$$

$$\begin{aligned} {}^{0}P_x &= l_1\cos(\theta_{11}) + l_2\cos(\theta_{11}+\theta_{12}) + l_3\cos(\theta_{11}+\theta_{12}+\theta_{13}) \\ {}^{0}P_y &= l_1\sin(\theta_{11}) + l_2\sin(\theta_{11}+\theta_{12}) + l_3\sin(\theta_{11}+\theta_{12}+\theta_{13}) \end{aligned} \tag{9}$$

The answer to the inverse kinematic analysis problem, which seeks an answer to the question of what leg joint angles should be for a desired leg end point position $({}^0P_x, {}^0P_y)$ defined in the leg fixed axes set, is as in equation 9. Here, an inverse kinematic analysis has been carried out so that the last lims of legs can hold the rails comfortably, so that the orientation of the last limb of legs always points towards the ground. For this reason, $\frac{3\pi}{2}$ value has been determined as a reference in the calculation of θ_{13}. Calculation of all three joint angles of the legs is obtained as in equation 10.

$$\cos(\theta_{13}) = ({P_x}^2(P_y + l_3)^2 - {l_2}^2)/2l_1l_2 \quad (10a)$$

$$\sin(\theta_{13}) = \sqrt{(1 - (cos(\theta_{13}))^2)} \quad (10b)$$

$$\theta_{11} = atan2(P_y + l_3), P_x) - atan2(k_1, k_2) \quad (10c)$$

Here, $k_1 = l_1 + l_2 \cos(\theta_{13})$ and $k_2 = l_2 \sin(\theta_{13})$

$$\theta_{12} = atan2(\sin(\theta_{13}), \cos(\theta_{13})) \quad (10d)$$

$$\theta_{13} = \frac{3\pi}{2} - \theta_{11} - \theta_{12} \quad (10e)$$

Here, the values for θ_{11}, θ_{12} and θ_{13} calculated for the left front leg, and these values are the same for the right front leg. For the rear legs, the variables θ_{21}, θ_{22} and θ_{23} are used, and in the calculation of these angles, since the structures of all legs are the same, the same inverse kinematic equations are used. However, in stage 2, the calculation of the angles of the joints of the hind legs is different with the calculation of the front legs. Because during this movement, the kinematic chain of the front legs and the rear legs are opposite [28]. In other words, in both leg groups, the calculation is made with the base axis set and the end axis set displaced.

The approach used to the walking strategy is discussed in the next section.

3. Results

3.1. Motion planning

In this section, motion planning of the robot is explained. The robot performs two basic movements on the greenhouse roof. The first is its movement with wheels on the iron bars while cleaning, which is relatively simple. During this movement, the robot moves forward or backward only along the iron bars with the help of wheels sitting on iron bars. In the other movement, the robot uses the legs it has to move to the other column after cleaning the column it is in.

The second movement, which is relatively complex, is planned in stages. It is desired that the orientation of the robot body does not change during the movement, because a simple but safe trajectory must be followed in order not to damage the additional components mounted on the robot for cleaning and to prevent the greenhouse glass from being damaged. In the rest of the section, the stages of movement planning for column change are explained in more detail. First of all, the legs end waiting idle in a predetermined position should be fixed to the iron bars in order to carry the body during column change. For this, as a first stage, the legs (front legs) in the direction of the new column that the robot will pass through must be fixed to the next iron bar in the direction of movement. Also, at this stage, the other legs (rear legs) should be fixed to the iron bars where the robot is located in order to prepare the task of moving the robot body from wheels to legs.

In the second stage, when the task of moving the robot body passes to the legs, the legs must lift the robot body without changing its orientation and move it to the next column. In the final stage, the legs should return to their original position so that they do not interfere with work during the cleaning task. The kinematic equations of these stages and the determined trajectories are given below.

Stage 1

At this stage, the trajectory that the legs should follow is determined as shown in the figure. Since the trajectory definition is made according to the **0** axis set fixed to the first joint of the legs, the inverse kinematic solutions obtained in equation 10 is used at this stage. As stated in the previous section, an inverse kinematic analysis has been made so that the orientation of the last limb (l_3) of the leg along the trajectory is always pointing downward so that the last limbs can be fixed to the bars. In Figure 7 the trajectories of the leg end points in the first and third stages are given. Here, $\hat{\mathbf{0}}$ is located at any point in the trajectory of motion of the end point of the last limb of the legs.

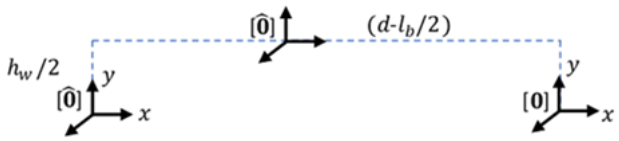

Figure 7. Legs end point trajectory of the robot

This trajectory consists of the movement of the leg joints in n_d steps. The position of the leg end point for each stage is calculated with equation 11. Where n_d is the number of steps $(n = 1 \ldots . n_d)$. ${}^{\hat{0}}P_x^*$ and ${}^{\hat{0}}P_y^*$ are desired position of legs end points.

$$\begin{aligned} {}^{\hat{0}}P_x^*(n) &= {}^0P_x(n_d) - (n * (d - l_b/2)/\, n_d \\ {}^{\hat{0}}P_y^*(n) &= {}^0P_y(n_d) - (n * h_w/2)/\, n_d \end{aligned} \quad (11)$$

Here, after the robot legs complete their movement in the y-axis, it starts its movement in the x-axis.

Stage 2

At this stage, the trajectory that the robot's body should follow is shown as in Figure 8. The trajectory

definition is made on the ***G*** axis set fixed to the body, so that the spatial position of the robot body does not need to be followed continuously. With this approach, kinematic calculations can be made without the need to know the spatial position of the robot during column change and a general control approach can be obtained. Here, the most important points are that the trajectory that the trunk should follow must be defined on the ***G*** axis set, the leg ends are fixed on the rails and the orientation of the body along the trajectory is fixed.

With this approach, the question of how the leg joints should change in order for the trunk to follow the desired trajectory should be answered while the positions of the leg end are fixed in space with respect to the ***G*** axis set. For this, first the positions of the leg ends should be determined according to the ***G*** axis set, then the inverse kinematic calculations should be made by calculating the positions in the $\hat{\boldsymbol{G}}$ axis set moved to any point on the trajectory.

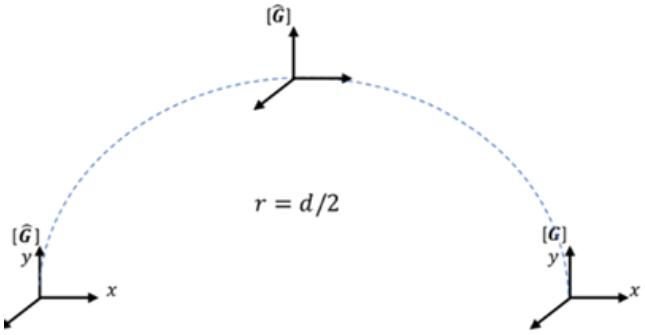

Figure 8. Body trajectory of the robot

The mathematical equivalents of these expressions are given in equations 12-18. An example of the location of the leg end points is shown for the left front leg (LF), and a similar calculation is made for the other legs. With Equation 12, the location of the leg end point with respect to the ***G*** axis set is found.

$$ {}^{G}_{3}T^{LF} = {}^{G}_{0}T^{LF} * {}^{0}_{3}T \tag{12} $$

${}^{\hat{G}}P_x^*$ and ${}^{\hat{G}}P_y^*$ are desired position of robot body along the trajectory in Equation 13.

$$ {}^{\hat{G}}P_x^* = (d/2) * (1 - \cos(n * pi/n_d) \tag{13a} $$

$$ {}^{\hat{G}}P_y^* = (d/2) * \sin(n * pi/n_d) \tag{13b} $$

Since there is no movement in z direction;

$$ {}^{\hat{G}}P_z^* = 0 \tag{13c} $$

And the planar trajectory;

$$ T_{trans} = [{}^{\hat{G}}P_x^* \ {}^{\hat{G}}P_y^* \ {}^{\hat{G}}P_z^*] \tag{14} $$

Thus, homogeneous transformation matrix in constant orientation is

$$ {}^{\hat{G}}T_G = \begin{bmatrix} I_{[3x3]} & T_{trans}^T \\ 0_{[1x3]} & 1 \end{bmatrix} \tag{15} $$

Since the body is rigid;

$$ {}^{\hat{G}}_{\hat{0}}T^{LF} = {}^{G}_{0}T^{LF} \tag{16} $$

In Equations 17-18, the location of the leg end point with respect to the $\hat{\boldsymbol{G}}$ axis set is found.

$$ {}^{\hat{0}}_{3}T^{LF} = \left[{}^{\hat{G}}_{\hat{0}}T^{LF}\right]^{-1} * \left[{}^{\hat{G}}T_G\right]^{-1} * {}^{G}_{3}T^{LF} \tag{17} $$

$$ \begin{aligned} {}^{\hat{0}}P_x^*(n) &= {}^{\hat{0}}_{3}T^{LF}(1,4) \\ {}^{\hat{0}}P_y^*(n) &= {}^{\hat{0}}_{3}T^{LF}(2,4) \end{aligned} \tag{18} $$

Stage 3

At this stage, the inverse kinematic solutions obtained in equation 10 is used again. Since there are similar movements as in seen Figure 7, the approach in Stage 1 was followed in the action planning of this stage.

$$ \begin{aligned} {}^{\hat{0}}P_x^*(n) &= {}^{\hat{0}}P_x(n_d) + (n * (d - l_b/2)/\, n_d \\ {}^{\hat{0}}P_y^*(n) &= {}^{\hat{0}}P_y(n_d) + (n * h_w/2)/\, n_d \end{aligned} \tag{19} $$

3.2. Walking simulation of the robot

The robot has two different movements on the greenhouse. One of these movements is carried out by four wheels on the robot body, which are driven by electric motors, on iron bars. This movement of the robot on the iron bars is realized only with the back-and-forth command given by the user. For this reason, this movement has not been simulated. Moving to the next column is a more important move. Which is the reason for the robot proposed in this study. This movement takes place with four legs. The results obtained from the simulation of this four-legged robot are given in this section. The physical properties of the robot used in the simulation are given in Table 1. These values can be changed for greenhouses with different dimensions.

Table 1. Cleaning robot specifications used in the simulation

Parameter	Dimensions [mm]						
	d	h_w	l_b	l_1	l_2	l_3	n_d
Value	550	200	50	400	400	100	20

The walking motion that the robot performs with four legs can be shown in three parts. When the robot moves on the rails with wheels, the four legs of the robot are in a position determined as the starting position as seen in Figure 9. First, the robot is fixed in a certain orientation of end limb on the iron bar in the next column by extending its two legs in the direction it should go. In the meantime, the two legs, which are opposite to the direction of movement of the robot, are fixed with a certain orientation to the iron bars on which the wheels closest to it are located.

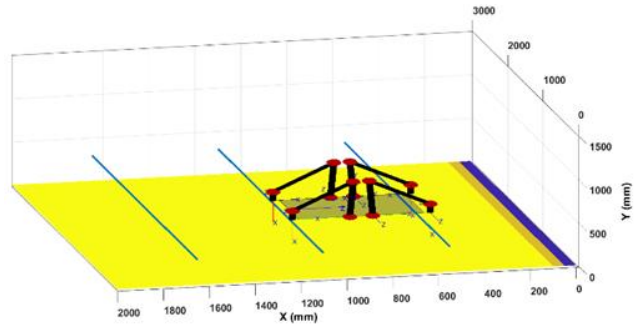

Figure 9. Starting position limbs of robot legs

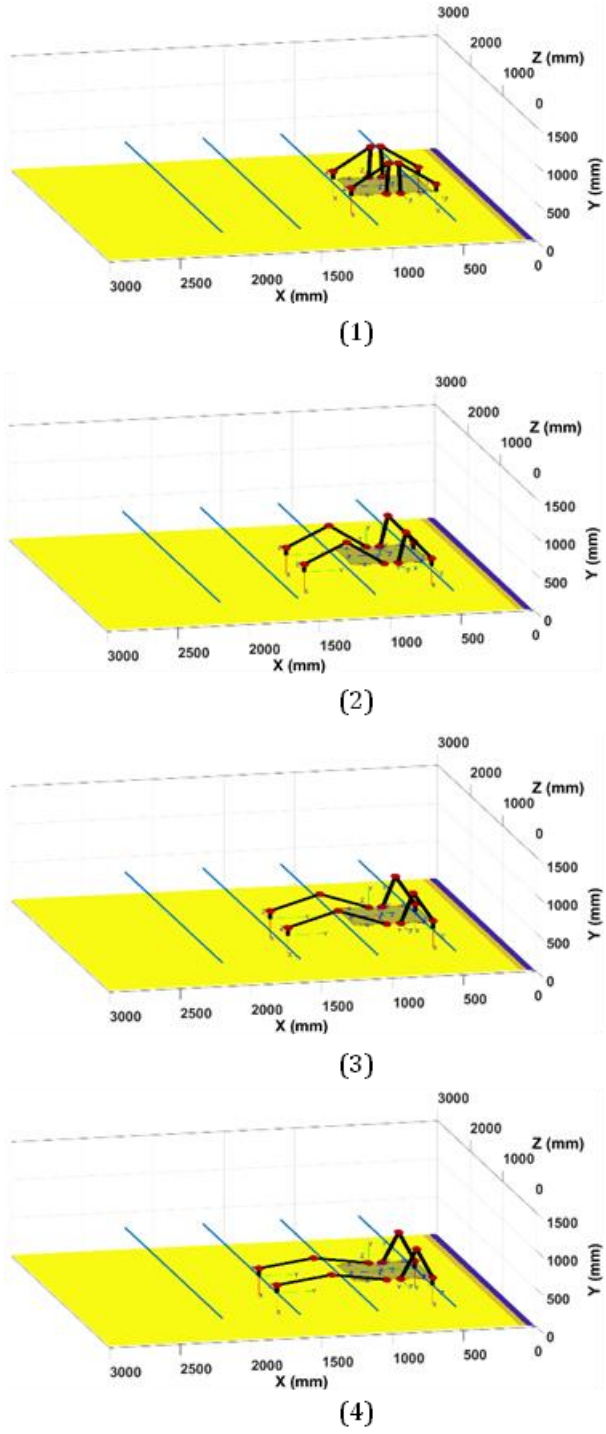

Figure 10. Stages of legs in first motion

After that, the robot's body is ready to move to the next column. The simulation images regarding this movement are given in Figure 10 in several steps.

The second movement is to move the robot body. In this walking movement, the two legs in the direction of the robot body move both by lifting and pulling the body of the robot, while the other two legs lift and push the body. These two movements occur synchronously without changing the angle of the robot body in any way. In the simulation, a trajectory is determined such that the robot body follows a half circle with a radius of 275 mm as seen in Fig. 8. In this walking action, the symmetry of the movement of the first two legs mentioned above is carried out by the other two legs.

Kinematically, these two groups of legs can be expressed as if the last limb and the first limb were replaced. The representation of this walking motion in eight states is given in Fig. 11 and Fig. 12.

The stages for this movement can be seen in Fig. 13. After the three stages of the robot's walking take place, the robot begins to move on the iron bars in the column it is located, by means of wheels, in order to clean the glass in the column where it is located.

4. Conclusion

In this study, a four-legged robot was designed and simulated for cleaning glass on the roof of greenhouses. The simulation study performed according to the mathematical model obtained showed that this proposed robot model can be used theoretically. This study, which focuses on the movement of the robot walking on the iron bars in order to pass to next column, also includes the movement of the robot with its wheels on the iron bars. However, since this movement is relatively simple and it is foreseen that it will be performed with the user command, it has not been emphasized much.

Four basic products have been found in the literature on robots and mechanisms designed or produced for glass cleaning. The first of these is the mechanisms that work with the principle of elevator on the building surface, developed for cleaning the glazed surfaces of high-rise buildings and the glazed parts of the windows.

The second is four-legged robots that can walk on vertical surfaces with the vacuum structure at their feet. The movement of these robots takes place by moving only one foot at each stage of walking. Using this walking strategy, the robot can move on this vertical surface without falling. Third, in which there is no walking motion, a rail structure is placed on the roof of the greenhouses, on which the washing mechanism can move with its wheels. The washing mechanism moves linearly on the rail on the roof of the greenhouse by performing the washing process towards the other end of the greenhouse. To clean the glass of another roof of the same greenhouse or the glass of the roof of another greenhouse, the rail structure and the washing mechanism must be reinstalled. Or, for this task, as many of these mechanisms as necessary should be installed for each roof and each greenhouse. The last one is robots developed for easier cleaning of dust on photovoltaic panels in solar power plants. These robots perform the cleaning task by moving on a fixed rail. Rail structure

installation is required in order to be used in a different solar power plant.

However, the robot proposed in this study can be used to clean glass on the roof of the greenhouse without any preliminary preparation. This robot can move between the grids in parallel with the determined walking strategy. For the cleaning task, by using the grids as a rail structure, it can move from the beginning to the end of the grid thanks to its wheels. The robot completes its task with these two basic movements. It has been designed with the motion strategy, which is a mixture of robots and mechanisms mentioned above, presented in the literature. It has been seen by the carried-out design, analysis and simulation that this robot can be used for cleaning the glasses of greenhouse roofs.

This proposed robot can be improved by performing both dynamic analysis and mechanical optimizations. In addition, it can be understood that it can be a final product by conducting tests in real environments with an experimental study.

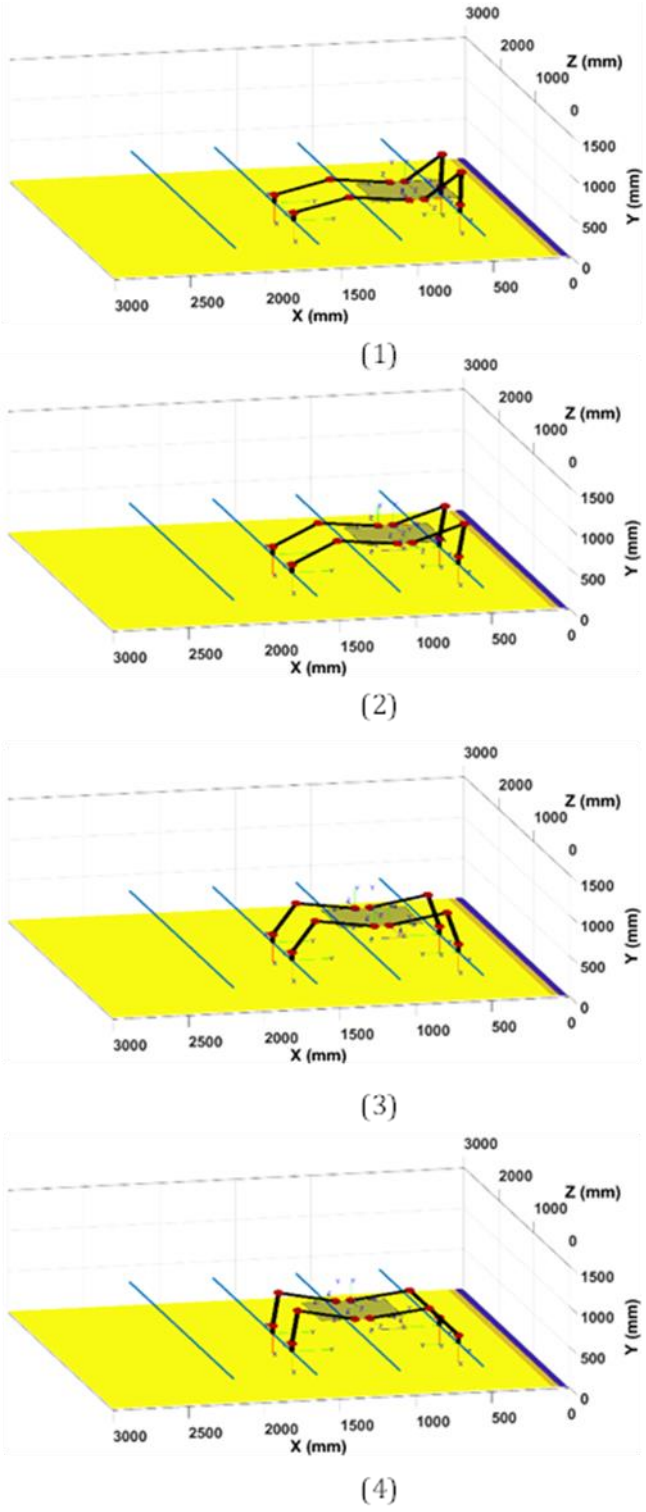

Figure 11. Walking states of robot for move body to next column (a)

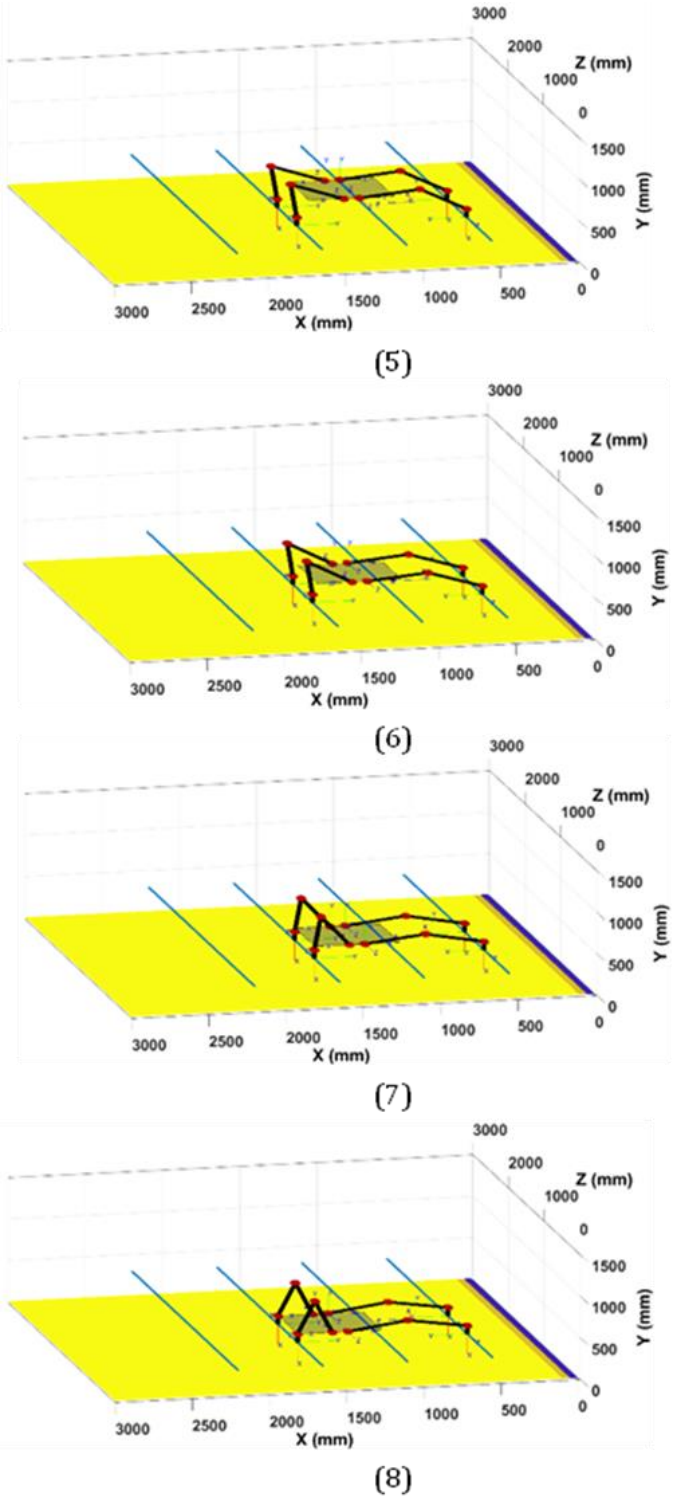

Figure 12. Walking states of robot for move body to next column (b)

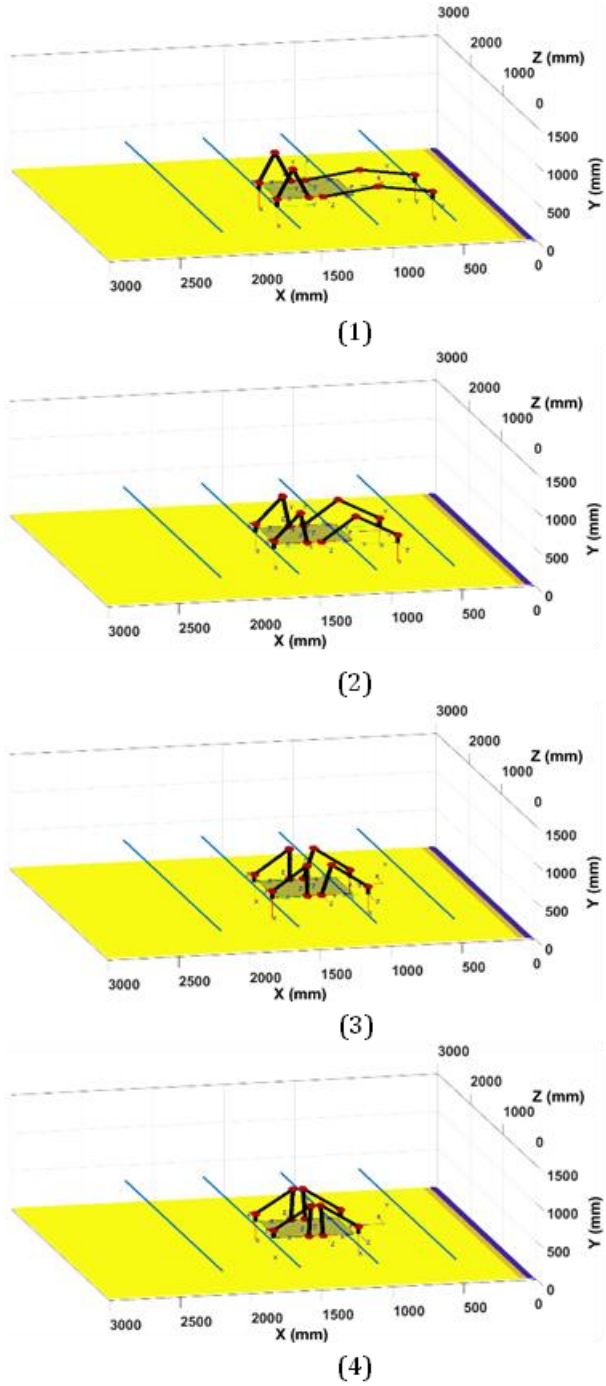

Figure 13. Motion stages of legs in last motion to arrive starting position

Conflicts of interest

The authors declare no conflicts of interest.

References

1. He, B., Cao, X., & Gu, Z. (2020). Kinematics of underactuated robotics for product carbon footprint. *Journal of Cleaner Production*, *257*, 120491.
2. Li, J., Wang, J., Peng, H., Zhang, L., Hu, Y., & Su, H. (2020). Neural fuzzy approximation enhanced autonomous tracking control of the wheel-legged robot under uncertain physical interaction. *Neurocomputing*, *410*, 342-353.
3. Li, J., Wang, J., Wang, S., Peng, H., Wang, B., Qi, W., Zhang, L., & Su, H., (2020). Parallel structure of six wheel-legged robot trajectory tracking control with heavy payload under uncertain physical interaction. Assembly Automation, 40, 675–687.
4. RunBin, C., YangZheng, C., Lin, L., Jian, W., & Xu, M. H. (2013). Inverse kinematics of a new quadruped robot control method. *International Journal of advanced robotic systems*, *10*(1), 46.
5. Shim, H., Yoo, S. Y., Kang, H., & Jun, B. H. (2016). Development of arm and leg for seabed walking robot CRABSTER200. *Ocean Engineering*, *116*, 55-67.
6. Wang, Z., Ding, X., Rovetta, A., & Giusti, A. (2011). Mobility analysis of the typical gait of a radial symmetrical six-legged robot. *Mechatronics*, *21*(7), 1133-1146.
7. Yıldırım, Ş., & Arslan, E. (2019). A Comparison of six legged ODE (open dynamics engine) based gait control algorithm and standard walking gaits. *Avrupa Bilim ve Teknoloji Dergisi*, 242-255.
8. Chen, J., Qiang, H., Wu, J., Xu, G., & Wang, Z. (2021). Navigation path extraction for greenhouse cucumber-picking robots using the prediction-point Hough transform. *Computers and Electronics in Agriculture*, *180*, 105911.
9. Tian, Y., Zhang, D., Yao, Y. A., Kong, X., & Li, Y. (2017). A reconfigurable multi-mode mobile parallel robot. *Mechanism and Machine Theory*, *111*, 39-65.
10. Ayyıldız, M., & Çetinkaya, K. (2016). Comparison of four different heuristic optimization algorithms for the inverse kinematics solution of a real 4-DOF serial robot manipulator. *Neural Computing and Applications*, *27*(4), 825-836.
11. Deng, H., Xin, G., Zhong, G., & Mistry, M. (2018). Object carrying of hexapod robots with integrated mechanism of leg and arm. *Robotics and Computer-Integrated Manufacturing*, *54*, 145-155.
12. Ghergan, O. C., Ţucu, D., Iusco, A., Drăghicescu, D., & Merce, R. M. B. (2019). Small greenhouse robotized solutions: state of the art and future perspectives. In *Proceedings of the 47th International Symposium, Actual Tasks on Agricultural Engineering, 5-7 March 2019, Opatija, Croatia* (pp. 267-276). University of Zagreb, Faculty of Agriculture.
13. Jia, B., Zhu, A., Yang, S. X., & Mittal, G. S. (2009, December). Integrated gripper and cutter in a mobile robotic system for harvesting greenhouse products. In *2009 IEEE International Conference on Robotics and Biomimetics (ROBIO)* (pp. 1778-1783). IEEE.
14. Roshanianfard, A., & Noguchi, N. (2020). Pumpkin harvesting robotic end-effector. *Computers and Electronics in Agriculture*, *174*, 105503.
15. Ling, X., Zhao, Y., Gong, L., Liu, C., & Wang, T. (2019). Dual-arm cooperation and implementing for robotic harvesting tomato using binocular vision. *Robotics and Autonomous Systems*, *114*, 134-143.
16. Martínez, D., Alenya, G., & Torras, C. (2015). Planning robot manipulation to clean planar surfaces. *Engineering Applications of Artificial Intelligence*, *39*, 23-32.
17. Hong, J., Yoo, S., Joo, I., Kim, J., Kim, H. S., & Seo, T. (2019). Optimal parameter design of a cleaning device for vertical glass surfaces. *International*

Journal of Precision Engineering and Manufacturing, *20*(2), 233-241.
18. Sun, D., Zhu, J., Lai, C., & Tso, S. K. (2004). A visual sensing application to a climbing cleaning robot on the glass surface. *Mechatronics*, *14*(10), 1089-1104.
19. Antonelli, M. G., Zobel, P. B., De Marcellis, A., & Palange, E. (2020). Autonomous robot for cleaning photovoltaic panels in desert zones. *Mechatronics*, *68*, 102372.
20. Li, T., Chen, D., Shi, G., Wei, M., Zhang, Y., & Chang, J. (2019). Analysis and suggestions of greenhouse cleaning machine in China and abroad. In *MATEC Web of Conferences* (Vol. 272, p. 01051). EDP Sciences.
21. Seemuang, N. (2017, April). A cleaning robot for greenhouse roofs. In *2017 2nd international conference on control and robotics engineering (ICCRE)* (pp. 49-52). IEEE.
22. Bakırcıoğlu, V., & Kalyoncu, M., (2019). A Literature Review on Walking Strategies of Legged Robots. Journal of Polytechnic, 0900, 961–986.
23. Çabuk, N., & Bakırcıoğlu, V. (2018). Altı serbestlik dereceli bir aydınlatma manipülatörünün yapay sinir ağları temelli ters kinematik çözümü ve benzetimi. *Gazi Üniversitesi Fen Bilimleri Dergisi Part C: Tasarım ve Teknoloji*, *6*(1), 117-125.
24. Dewi, T., Nurmaini, S., Risma, P., Oktarina, Y., & Roriz, M. (2020). Inverse kinematic analysis of 4 DOF pick and place arm robot manipulator using fuzzy logic controller. *International Journal of Electrical & Computer Engineering*, *10*(2), 1376–1386.
25. Pellicciari, M., Berselli, G., Leali, F., & Vergnano, A. (2013). A method for reducing the energy consumption of pick-and-place industrial robots. *Mechatronics*, *23*(3), 326-334.
26. Şen, M. A., Bakırcıoğlu, V., & Kalyoncu, M. (2020). Three degree of freedom LEG desıgn for quadruped robots and fractıonal order PID (PIλDμ) based control. *Konya Mühendislik Bilimleri Dergisi*, *8*(2), 237-247.
27. Yildirim, Ş. (2008). Design of a proposed neural network control system for trajectory controlling of walking robots. *Simulation Modelling Practice and Theory*, *16*(3), 368-378.
28. Yildirim, Ş. (2005). A proposed hybrid recurrent neural control system for two co-operating robots. Journal of Intelligent and Robotic Systems, 42(1), 95-111.